DELPHI 97-74 CONF 60
28 July, 1997

m_b at M_Z

Preliminary

DELPHI Collaboration

S. Cabrera, J. Fuster
IFIC, Avda. Dr. Moliner 50, E-46100 Burjassot-Valencia, Spain
S. Marti
Oliver Lodge Laboratory, Physics Department, Univ. of Liverpool
Oxford Street, Liverpool L69 7ZE, U.K.

Abstract

The value of the b quark mass at the M_Z scale defined in the $\overline{MS}$ renormalization scheme, $m_b(M_Z)$, was determined using 2.8 million data events collected during the years 1992, 1993 and 1994 by the DELPHI collaboration at the Z peak. The obtained result is

$$m_b(M_Z) = 2.67 \pm 0.25 \text{ (stat.)} \pm 0.34 \text{ (frag.)} \pm 0.27 \text{ (theo.) } GeV.$$

This analysis, performed at an energy far from the $b\bar{b}$ production threshold, confirms the running of the b-quark mass and establishes the first experimental evidence of the running of any fermion mass.

Paper submitted to the LP'97 Conference
Hamburg, July 28 - August 1st

1 Introduction

In the Standard Model (SM) of the strong (QCD) and electroweak (EW) interactions the masses of all the fermions, leptons and quarks, are described as fundamental free parameters. From the perspective of the SM Lagrangian the mass parameters are effective coupling constants which can be included in the renormalization procedure of the theory. As is well known, several valid renormalization schemes exist, each one postulating different renormalized mass definitions. The perturbative pole mass, M_q, and the running mass, m_q, of the $\overline{MS}$ scheme are mass definitions among the most attractive due to their intrinsic physical properties. The former definition is the renormalized pole of the fermion propagator and is scheme invariant though naturally prescribed by the on-shell scheme. For free fermions, it corresponds to the usual kinematic mass reconstructed in the experiments. The latter definition is purely dynamical, it is associated to the renormalized fermion mass of the $\overline{MS}$ scheme and depends on the energy scale of the process under study, μ. This last feature, which is not shared by the pole mass, has never been cross-checked with experiment even though its confirmation takes deep roots on the renormalizable structure of the SM theory and has important implications on the unification of the so called Yukawa couplings.

Heavy fermions show the strongest absolute dependence of the running mass with the energy scale and hence they are the best candidates to test the *running mass* property. At LEP energies this statement sets up the b-quark mass as the experimental target of such an analysis and QCD as the proper theoretical scenario. Mass determinations are, in general, more complicated and less precise for quarks than for leptons. This is due to the fact that stable quarks only exist composing bound states and the use of dynamical relations to unfold the strong bounding forces between the quarks is mandatory. Up to now, the b quark mass is extracted from the known spectra of the hadronic bound states of the Υ resonances by using, e.g., QCD sum rules or lattice calculations [1]. The b pole mass measured with these methods is $M_b \approx 4.7$ GeV and the b running mass is $m_b(m_b) \approx 4.2$ GeV at $\mu = m_b$. The QCD predicted change of this value at the LEP energy scale is of the order of $(m_b(m_b) - m_b(M_Z)) \sim +1.2$ GeV.

At LEP energies, $\sqrt{s} \gtrsim M_Z$, b quark mass effects usually appear in terms proportional to m_b^2/M_Z^2 ($\lesssim 3‰$) and can be safely neglected for many observables, as for instance for the total hadronic cross section. On the other hand, for other specific quantities, like the differential multi-jet cross section for b events, the mass corrections lead to sizeable contributions because in these expressions they are of the form $m_b^2/M_Z^2/y_c$ with y_c being the jet-resolution parameter ($\sim$0.01). Earlier calculations including mass terms already exist at Leading Order (LO) for three- and four-jet event rates [2, 3] and have been used in the test of the universality of the strong coupling constant for b events, α_s^b. A suppression factor of the order $\sim$5% [2, 3, 4] is predicted for the three-jet cross section of events originated by b quarks with respect to that of events initiated by light quarks ($\ell \equiv u, d, s$). The exact value of this factor depends of course on m_b, y_c and the chosen jet reconstruction algorithm. However these calculations could not be used to evaluate m_b itself, because they only contain LO terms with no need of any particular renormalization processing. As no renormalization information was required, no physical argument could then be developed to consistently identify the mass parameter appearing in these expressions as being either the pole or the running mass. Only, recently, Next to Leading Order (NLO) calculations have become available for the multi-jet production rate [5, 6, 7, 8]. They solve this mass ambiguity as they include radiative loop corrections and, thus, enable a proper determination of m_b. The proposed measurable quantity is [4, 6, 9]:

$$R_3^{b\ell}(y_c) = \frac{\Gamma_{3j}^{Z\to b\bar{b}g}(y_c)/\Gamma_{tot}^{Z\to b\bar{b}}}{\Gamma_{3j}^{Z\to \ell\bar{\ell}g}(y_c)/\Gamma_{tot}^{Z\to \ell\bar{\ell}}} = 1 + r_b(\mu)\cdot\left(b_0(y_c, r_b(\mu)) + \frac{\alpha_s(\mu)}{\pi}\cdot b_1(y_c, r_b(\mu))\right) \qquad (1)$$

where $\Gamma_{3j}^{Z\to q\bar{q}g}$ and $\Gamma_{tot}^{Z\to q\bar{q}}$ are the differential three-jet and total cross sections, respectively, for the b ($q = b$) and light ($q = \ell \equiv u, d, s$) quarks. The parameter $r_b(\mu)$ is $m_b^2(\mu)/m_Z^2$ and b_0 and b_1 are functions which can be found in reference [6].

In this letter the DELPHI measurement of m_b is presented at LEP scales using $R_3^{b\ell}$ as the direct observed quantity and equation 1 as the expression to extract m_b at M_Z. The comparison of this result with the value of m_b obtained from the Υ resonances represents the first experimental attempt to establish the *running property* of the b quark mass, in particular, and of any fermion mass, in general.

2 Detector description

The DELPHI detector, surrounding one of the interaction regions at the Large Electron Positron facility LEP at CERN, has been used to record the samples of events considered in this analysis. It provides both tracking and calorimetric information over almost the full solid angle. A detailed description of the detector, the exact geometry as well as the trigger conditions and the event processing chain appear in reference [10].

The barrel region of the detector consists of a system of cylindrical tracking detectors and an electromagnetic calorimeter, embedded in a superconducting solenoidal coil providing a uniform magnetic field of 1.23 T parallel to the beam direction (z). The central tracking detectors, Vertex Detector (VD), Inner Detector (ID), Time Projection Chamber (TPC) and Outer Detector (OD), provide measurements of charged particles in both the $r\phi$ plane, transverse to the beam, and in the z direction. The VD consists in three concentric layers of silicon microstrip detectors. In 1994 this detector was upgraded and two of the layers were replaced by double sided silicon microstrip detectors. The ID is a cylindrical jet chamber surrounded by five layers of multi-wire proportional chambers. The TPC is the main tracking device, that also provides information on energy loss, dE/dx. The tracking in the barrel region is completed by the OD which is composed of five layers of drift cells and in the endcaps by further tracking Forward Chambers, FCA/B. The DELPHI tracking system provides an average momentum resolution of $\sigma(p)/p = 3.6\%$ for muons of 45 GeV/c.

The electro-magnetic calorimetry is accomplished by the High Density Projection Chamber (HPC) and the Forward Electromagnetic Calorimeter (FEMC) that correspond to the barrel and forward region, respectively. Their information allows identifying electrons and photons. The muon identification is performed by the muon detector system that consists of several layers of drift chambers and is located within and beyond the outer layers of the hadron calorimeter (HAC) which also serves as the return yoke of the magnet.

3 Event selection

All data collected by DELPHI during 1992, 1993 and 1994 were considered in the present analysis and corresponded to center-of-mass energies of $\sqrt{s} \approx M_Z$. In a first step of the selection procedure, quality cuts on all charged particles and all neutral clusters in the calorimeters were imposed in order to ensure a reliable determination of their kinematic variables, momenta and energies. The charged particles entering in the analysis were all assumed to be charged pions and required to be well contained within the detector acceptance and to have large enough momenta to guarantee a good track reconstruction and originating close to the interaction point (IP). Neutral clusters reconstructed in the HPC, FEMC and HAC were selected by imposing conditions on the minimum reconstructed energy, with an additional requirement on the distribution of the layers hit for HPC clusters. Identified electron positron pairs arising from photon conversions were considered as single neutral clusters if the sum of their momenta exceeded 600 MeV/c.

A sample of hadronic events was then selected by demanding a minimum charged multiplicity, enough visible charged energy and being well contained within the detector volume, with a veto on those events having mismeasured particles. The retained data sample fulfilling the hadronic criteria contained $\sim 2.5 \cdot 10^6$ events with a small contamination arising from $\tau^+\tau^-$ pairs ($\sim$1‰) and negligible background from beam-gas scattering and $\gamma\gamma$ interactions. In table 1 the specific cuts used at this stage are presented.

Charged Particle Selection	p$\geq$ 0.1 GeV, Δ(p)/p$\leq$1 $25° \leq \theta \leq 155°$ L$\geq$ 50 cm $\delta \leq$ 5 cm in $r\phi$ plane $\delta \leq$ 10 cm in z plane	
Neutral Cluster Selection	$E \geq 0.8$ GeV, $40° \leq \theta \leq 140°$ $E \geq 0.5$ GeV, $8°(144°) \leq \theta \leq 36°(172°)$ $E \geq 1.5$ GeV, $10° \leq \theta \leq 170°$	HPC FEMC HAC
Event Selection	$N_{ch} \geq 5$ $E_{ch} \geq 15$ GeV $\lvert \sum_i q_i \rvert \leq 6$, i=1,..,$N_{ch}$ No particle with $E \geq 40$ GeV $40° \leq \theta_{thrust} \leq 140°$	

Table 1: Particle and hadronic event selection; p is the particle momentum, θ the particle (or *thrust*) polar angle w.r.t beam axis, L the measured track length, δ the closest distance to the IP, q_i the particle charge, E the cluster energy, N_{ch} the number of charged particles and E_{ch} the total charged energy of the event.

The charged and neutral particles of every selected event were then grouped into jets by means of the DURHAM jet finding algorithm [11] whose definition and main properties appear in table 2. For each pair of particles ij, the DURHAM jet resolution variable y_{ij} was calculated from the corresponding four-momentum vectors of both particles. The pair with the smallest y_{ij} that did not exceed the resolution parameter, y_c, was recombined to form a new pseudo-particle with four-momentum as prescribed by the DURHAM scheme. The procedure was reiterated until no further pairs of particles or pseudo-particles satisfied the condition $y_{ij} \leq y_c$. The final remaining particles or pseudo-particles were henceforth referred to as jets and the number of such clusters determined the event class (two-jet, three-jet, etc..) to which every particular event was associated as a function of y_c.

Algorithm	Reference	Resolution	Recombination
DURHAM (k_T)	[11]	$y_{ij} = \frac{2 \cdot \min(E_i^2, E_j^2) \cdot (1 - cos\theta_{ij})}{E_{vis}^2}$	$p_k = p_i + p_j$

Table 2: Definition of the jet resolution variable y_{ij} of the DURHAM recombination scheme; E_{vis} is the total visible energy of the event, $p_i \equiv (E_i, \vec{p}_i)$ denotes a 4-vector and θ_{ij} is the angle between $\vec{p}_i$ and $\vec{p}_j$.

The sample of accepted events contained well identified hadronic events but their kinematics could still be affected by particle losses and wrong energy-momentum assignment to jets. In order to ensure a good energy balance of these hadronic events further quality cuts were applied using information of the reconstructed jets. For each event the maximum y_c value, which classified it as a three-jet, was determined. The jet energies were re-calculated using the relative angle separation between jets by means of the triangle relation reported in [12] and the set of conditions listed in table 3 were imposed. A total of $1.9 \cdot 10^6$ hadronic events passed these criteria and the $\tau^+\tau^-$ pair contamination was further reduced to be less than $0.01‰$.

Kinematic Selection	$N_{ch} \geq 1$ per jet $E_j \geq 3$ GeV $j = 1,2,3$ $25° \leq \theta_j \leq 155°$ $j = 1,2,3$ Planarity cut in the event plane: $\sum_n \phi_{ij}^n \geq 359.9°$, $i \neq j,\ i,j,n = 1,2,3$

Table 3: Event selection based on the kinematic properties of the events when clustered in three-jets by the DURHAM algorithm; E_j is the jet energy, θ_j is the jet polar angle and ϕ_{ij} the angular separation between the pair of jets ij in the event plane.

The signed impact parameter of charged particles was used to construct an algorithm for tagging b and ℓ events [13, 14] in an attempt to identify the original flavour of the individual events. In this method the probability, P, to contain no decay products from long lived hadrons was evaluated using all the selected charged tracks of the event that had positive impact parameter. Initiated b quark events gave small values of P whereas ℓ events showed an almost flat P distribution and hence, P, could be used to discriminate the flavour of the event. The $\mathrm{Log}_{10}(\mathrm{P})$ distribution is shown in figure 1 for real data and simulated events [15]. A good agreement between real and simulated data can be observed. The cut on P to select b candidates was fixed to P$\leq 5{\cdot}10^{-3}$ independently of the year in which the data were collected. Each value of P corresponds to a well determined combination of purity and efficiency [14] for either b or ℓ events. The achieved purity and efficiency were different for each year, though around 85% and 55% respectively. In the case of light quarks P was required to exceed 0.2 leading to about 80% purity, and, consequently to $\sim$ 80% efficiency. The final amount of data that survived all the above requirements is itemized in table 4 for the specific samples of b and ℓ initiated events. The average flavour composition of each sample, *i.e.*, the purity and the contamination, is also given in table 4 according to the results derived from the DELPHI detector simulation [15].

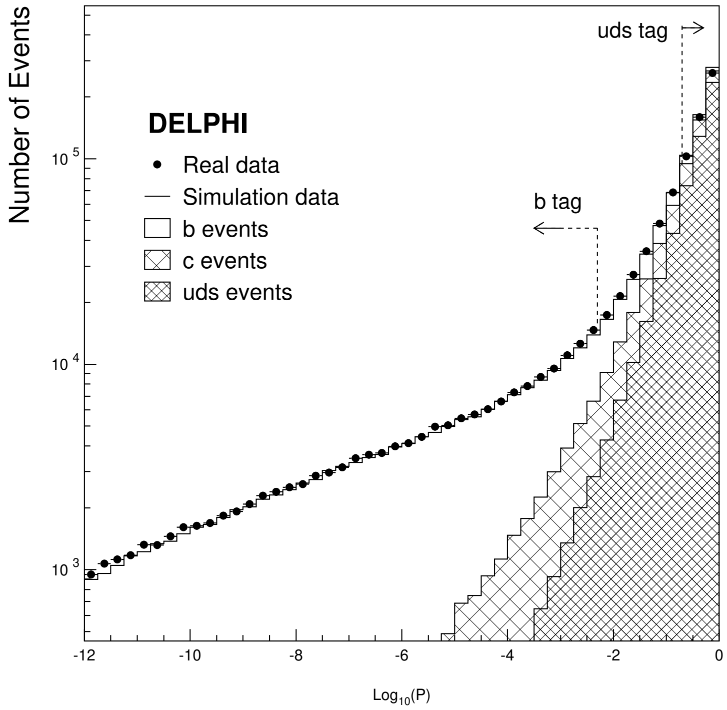

Figure 1: Event distribution of the logarithm of the probability to contain no secondary vertices (P). The 1994 real (points) and simulated data (solid line) are compared. The specific contribution of each quark flavour is displayed as derived from the simulation. The cuts used to tag the b and the light, $\ell \equiv u, d, s$, quark samples are also indicated.

# ev. in data	q-type	$\ell \to q$ (%)	$c \to q$ (%)	$b \to q$ (%)
1,074.860	ℓ	80.2 $\pm$ 1.8	15.1 $\pm$ 0.6	4.7$\pm$1.1
294.509	b	5.1 $\pm$ 0.3	10.1 $\pm$ 2.1	84.8 $\pm$2.4

Table 4: Final amount and flavour composition of the b and light, $\ell \equiv u, d, s$, tagged data

samples. The purities and the errors were extracted from simulation and corresponded to the average and standard deviation values obtained after gathering all years data.

4 Experimental strategy

The selected events were in their turn classified in two groups according to their tagged flavour. For each data set, the normalized measured three-jet cross section, $R_{3q}^{mes}(y_c) = \Gamma_{3j-mes}^{Z\to q\bar{q}g}(y_c)/\Gamma_{tot-mes}^{Z\to q\bar{q}}$ with $q \equiv b, \ell$, was computed as well as the ratio between both quantities,

$$R_3^{b\ell-mes}(y_c) \quad = \quad \frac{R_{3b}^{mes}(y_c)}{R_{3\ell}^{mes}(y_c)}$$

As usual, this measured value, obtained for the selected events, was corrected to account for detector acceptance effects, for kinematic biases introduced in the tagging procedure and for the hadronization process. This raw result had then be transformed into the quark-parton result equivalent to the theoretical expectation of equation 1. To perform this practice, a sample of $\sim 4 \cdot 10^6$ simulated events was employed. These data were generated using the JETSET 7.3 Parton Shower (PS) Monte Carlo [16] and passed the full simulation and reconstruction of DELPHI [15]. The same analysis as for the real data was applied to the simulated events and analogously the normalized three-jet cross sections were defined for each set of tagged events. In this case, however, the contribution of each quark flavour to the measured normalized three-jet cross section could be quantified according to

$$\begin{aligned} R_{3b}^{mes-sim}(y_c) &= R_{3b}^{b-sim}(y_c) \cdot c_b^b + R_{3b}^{\ell-sim}(y_c) \cdot c_b^\ell + R_{3b}^{c-sim}(y_c) \cdot c_b^c \\ R_{3\ell}^{mes-sim}(y_c) &= R_{3\ell}^{b-sim}(y_c) \cdot c_\ell^b + R_{3\ell}^{\ell-sim}(y_c) \cdot c_\ell^\ell + R_{3\ell}^{c-sim}(y_c) \cdot c_\ell^c \end{aligned} \qquad (2)$$

where $R_{3q}^{mes-sim}(y_c)$ was the simulated normalized three-jet cross section of each data sample equivalent to the measured quantity; $R_{3q}^{i-sim}(y_c)$ $(i = b, c, \ell)$, corresponded to the normalized three-jet cross section of each quark flavour and the weights, c_q^i, were the purity factors listed in table 4. The flavour assignment, i, of the events entering in the the terms, $R_{3q}^{i-sim}(y_c)$, was defined to be the flavour of the pair of quarks coupled to the Z which initiated the parton shower. This avoided flavour misidentification ambiguities due to the gluon splitting into quarks occurring during the parton shower evolution. The same convention was considered in the theoretical calculation of [6] and therefore a consistent comparison was allowed for.

Detector effects, acceptance plus kinematic biases, $g(y_c)$, and hadronization, $f(y_c)$, were then computed for each term of equation 2 as multiplicative factors connecting the normalized three-jet cross sections R_{3q}^{i-sim} with their related parton level quantities, R_{3q}^{i-par}, as

$$R_{3q}^{i-sim}(y_c) \quad = \quad f_{3q}^i(y_c) \cdot g_{3q}^i(y_c) \cdot R_{3q}^{i-par}(y_c).$$

The particular detector configuration of each year was considered in the correction procedure although the underlying physics involved in the hadronization process were assumed not to depend on the data collection date. Consequently, different $g(y_c)$ factors were calculated corresponding to each year as opposed to the $f(y_c)$ factors which were always kept the same and were taken from the tuned DELPHI parameters appearing in reference [17].

Effects due to the mass of the c quark were neglected as their size is about ten times lower than the one induced by the b quark mass, $\sim m_b^2/m_c^2$. Thus the normalized three jet cross section of c quarks at parton level was assumed to be equal to that of light quarks, *i.e.*, $R_{3q}^{c-par} = R_{3q}^{\ell-par}$. This allowed to relate the parton and the simulated *measured* quantities in the following way

$$\begin{aligned} R_{3b}^{mes-sim}(y_c) &= A_b(y_c) \cdot R_{3b}^{par}(y_c) + B_b(y_c) \cdot R_{3\ell}^{par}(y_c) \\ R_{3\ell}^{mes-sim}(y_c) &= A_\ell(y_c) \cdot R_{3b}^{par}(y_c) + B_\ell(y_c) \cdot R_{3\ell}^{par}(y_c) \end{aligned} \tag{3}$$

where the parameters A_b, B_b, A_ℓ, B_ℓ are a more compact re-definition of the original set of parameters: $f_{3q}^i, g_{3q}^i, c_{3q}^i$. The values of these parameters were then used to express $R_3^{b\ell-par}$ as a function of $R_3^{b\ell-mes}$ according to

$$R_3^{b\ell}(y_c) = R_3^{b\ell-par}(y_c) = \frac{R_{3b}^{par}(y_c)}{R_{3\ell}^{par}(y_c)} = \frac{B_b(y_c) - B_\ell(y_c) \cdot R_3^{b\ell-mes}(y_c)}{A_\ell(y_c) \cdot R_3^{b\ell-mes}(y_c) - A_b(y_c)} \tag{4}$$

which could then be compared to the theoretical prediction of equation 1.

The overall correction to the observed value of $R_3^{b\ell-mes}(y_c)$ was about 7% (averaged for all years) from which ~1% was due to the hadronization process. All years data sets after correction showed good agreement with each other within one standard deviation of the statistical error. Therefore, they were combined without further requirements. In figure 2 the corrected data distribution of $R_3^{b\ell-par}(y_c)$ obtained using equation 4 is shown together with the theoretical expectations at LO ($\mathcal{O}(\alpha_s)$) from references [2, 3] and at NLO ($\mathcal{O}(\alpha_s^2)$) from references [6, 7] for m_b mass values equal to 3 GeV and 5 GeV in both cases.

A high level of agreement between the two recent NLO calculations [6] and [7] is noticed even though both calculations use a slightly different definition of the observable $R_3^{b\ell}(y_c)$. In reality, however, only the events which have two reconstructed $b\bar{b}$-jets both originating from a splitted gluon do in fact contribute to such differences. The induced effect on R_3^{bl} was studied using the JETSET 7.3 generator. First it was checked that the perturbative calculations from [6, 18] were reasonably well described by the generator and, second, the effect on R_3^{bl} of reconstructing two separate $b\bar{b}$-jets produced by the same splitted gluon was evaluated. As a function of y_c the gluon splitting probability into two b-quarks lead to changes in R_3^{bl} of the order of ~(2-6)‰ which were compensated by the probability that both quarks be reconstructed. This probability varied from 30% to 15% depending again on y_c. The net effect was therefore below 1‰ and explains the nice agreement which is observed in figure 2 between the two curves of the two theoretical approaches. The data shown in figure 2 were also corrected to account for the contribution of anomalous triangle diagrams to the three-jet final state [19]. This contribution was about ~+2‰ for R_3^{bl}.

5 The systematics

The study of the systematic uncertainties was performed using principally the JETSET 7.3 event generator. This program contains mass effects based on LO perturbative calculations [20] which govern the emission of hard gluons and in the rest of the phase space

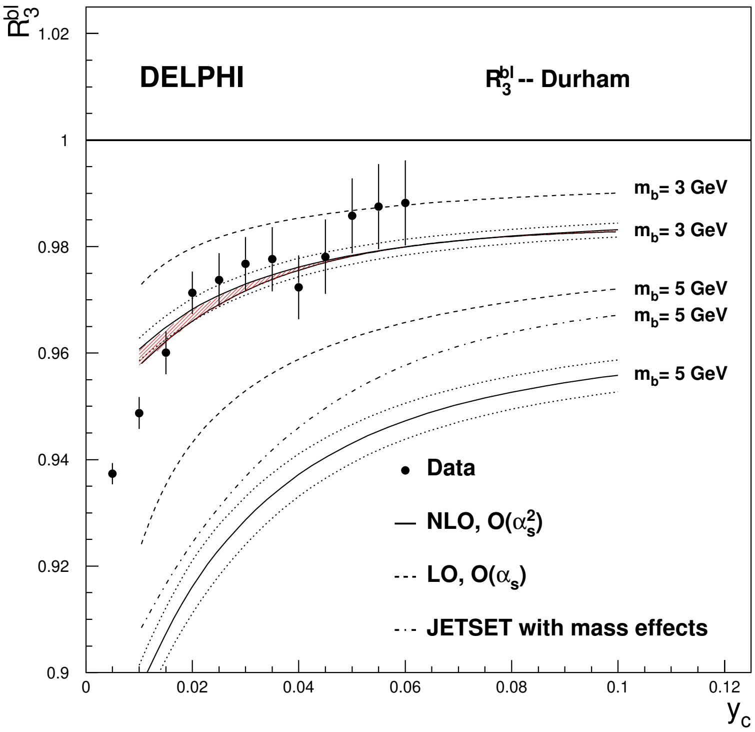

Figure 2: Distribution of $R_3^{b\ell-par}(y_c)$ for corrected data (black points) in comparison with the theoretical predictions. The dashed lines indicate the LO ($\mathcal{O}(\alpha_s)$) predictions from references [2, 3]. The solid lines are the NLO ($\mathcal{O}(\alpha_s^2)$) calculation of reference [6]. The dotted points contain the area corresponding to a scale interval of $0.5 \leq \mu/m_Z \leq 2$. The dashed area indicates the spread of predictions [6] and [7] for an identical value of m_b of 3 GeV. The dashed-dotted curve shows the JETSET behaviour for mb=5 GeV when mass effects are included.

only kinematics are considered. The default value of m_b employed by this program is 5 GeV which represents a sufficiently good approximation to describe data for most of the present LEP analyses. The predicted R_3^{bl} ratio by this model is also shown in figure 2.

The evaluation of the hadronization correction factors to R_3^{bl} by means of the O(α_s^2) ME (Matrix Element) expressions as they exist in JETSET was discarded because they use the masless approximation and, furthermore, in this scenario the multi-jet production rate after fragmentation is strongly influenced by the jet transverse momentum parameter σ_q which is the same for all flavours. On the contrary the Parton Shower (PS) option includes some more refined approximation to the massive approach and, in addition, σ_q is less relevant to the multi-jet production rate after fragmentation. The reliable use of the PS model in this analysis was however restricted to a y_c region where the two- and three-jet event rates are dominant. This was defined by requiring $y_c > 0.015$ which guaranteed that the four-jet production rate was lower than 2% and, still, the event statistics were relatively high.

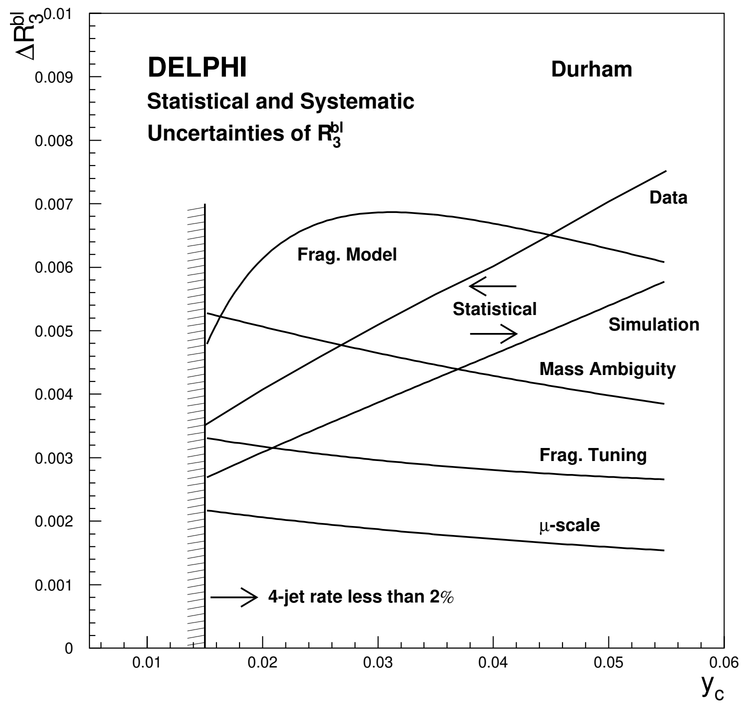

Figure 3: Statistical and systematic uncertainties affecting R_3^{bl} as a function of y_c. The Mass Ambiguityt and the μ-scale are not specific errors of R_3^{bl} but they are shown for comparison purposes.

The possible dependence of the applied correction factors with respect to the value of the b mass was also studied. With the present configuration of JETSET this was technically difficult as the program uses the same value of m_b to describe both hard and soft processes. A too small value of m_b could lead to unreliable results, as for instance, to unphysical B hadron decays. Still this feature could be tested indirectly by switching on and off the mass effects and evaluate the change, if any, of the correction factors. This exercise altered the proportion of three-jet b events at parton level while the fragmentation process kept its physical meaning. The number of three-jet b events after fragmentation was seen to scale with the corresponding number at parton level and, therefore, no variation of the correction factors was observed within the precision derived by the statistics produced, this being $\sim 1‰$.

The description of the parton shower evolution is also not unique and various schemes which describe reasonably well the data are possible. The distributions for R_3^{bl} obtained when correcting either by JETSET 7.3 PS [16] or by HERWIG 5.8 [21] were compared using samples of generated events that contained more than 10^7 events. Both programs were seeded with the best set of paramaters tuned by DELPHI [17] which are also in good agreement with those found by ALEPH [22]. The obtained corrected R_3^{bl} distributions using one or the other scheme differed by about 1%. The adopted correction value was then the average of both models and the error due to the uncertainty of the fragmentation model was assumed to be half of this difference. The data shown in figure 2 were corrected using this method and the dependence of the fragmentation model error as a function of y_c can be seen in figure 3.

Another source of systematics is induced by the lack of exact knowledge of the fragmentation parameters of JETSET. Again, huge samples of simulated events were generated (10^7 events per flavour: b and ℓ and per parameter) in order to study the particular effect of each JETSET parameter relevant to this analysis: Q_0, σ_q, ϵ_b, a and b. Each of these parameters was assumed to take the optimum value found in the DELPHI tuning and varied by $\pm 2\sigma$ from its central value. None of the individual uncertainties associated with the cited parameters affected the R_3^{bl} determination by more than 2‰ for y_c values in the region $y_c > 0.01$. The global error given in figure 3 was calculated by adding each individual contribution in quadrature neglecting the correlation. In this way, the error associated to the uncertainty of the tuned fragmentation parameters represented a conservative approach and it was calculated to be $\sim$3‰ .

The impact on R_3^{bl} of taking R_{3q}^{c-par} equal to $R_{3q}^{\ell-par}$ was found negligible.

The defects of the DELPHI detector modelling when trying to reproduce the real data were also considered in the analysis and regarded as an additional source of error. The main contribution to this uncertainty came from the limited statistics of the simulated events including the full detector and the purity/background factors of the b-tagged and ℓ-tagged samples. The size of this error was derived by solving equation 4 when the different flavour contribution (c_{3q}^q) were changed individually by 1% but keeping $\Sigma_q c_{3q}^q = 1$ and by calculating the statistical precision of the simulated sample. The overall error is shown in figure 3 and is dominated by the limited statistics available.

6 Results and discussion

The corrected $R_3^{b\ell}$ distribution is shown in figure 2 as a function of y_c. All data points at different y_c values are highly correlated and, therefore, the measurement of m_b was based on a single point. The optimization of the statistical error advised the use of small y_c values although they had to lay in a region in which the non-perturbative effects and the contributions due to multi-jet final states exceeding three-jets were kept small ($y_c > 0.015$). By taking the curves shown in figure 3 the y_c value that minimized the total error was chosen. A value of $y_c = 0.02$ was then adopted and this corresponded to the $R_3^{b\ell}$ value that is presented in table 5 together with the break down of the individual errors. This is

$$R_3^{b\ell}(0.02) = 0.971 \pm 0.005\ (\text{stat.}) \pm 0.007\ (\text{frag.}) \tag{5}$$

where the statistical error from the data and the simulation have been added up and the fragmentation error accounts for the uncertainties arising from the fragmentation model and the tuning parameters.

$y_c = 0.02$		
	R_3^{bl}	$m_b(M_Z)$ GeV
Value	0.971	2.67
Statistical error	± 0.004	± 0.20
Simulation error	± 0.003	± 0.15
Fragmentation Model error	± 0.006	± 0.30
Fragmentation Tuning error	± 0.003	± 0.15
Mass Ambiguity error	–	± 0.25
μ-scale error ($0.5 \leq \mu/m_Z \leq 2$)	–	± 0.10

Table 5: Values of $R_3^{b\ell}$ and $m_b(M_Z)$ and break down of their associated errors (statistical and systematic) for $y_c = 0.02$.

The theoretical uncertainties only enter when the measurement of R_3^{bl} is transformed into a determination of $m_b(M_Z)$ by means of equation 1. In figure 3 they are shown associated to R_3^{bl} for comparison purposes. As also happens for α_s measurements there is an unphysical scale dependence which needs to be quantified and, in addition to this, there is a *mass ambiguity* arising from the fact that two ways of expressing equation 1 in terms of the running b mass at the M_Z scale are allowed for [6, 23]. This latter uncertainty is labelled as the *mass ambiguity* in figure 3 and it reflects the ambiguity of writting equation 1 directly in terms of the running mass at the M_Z scale or using the pole mass as an intermediate stage, transform this mass to the running mass at the pole mass scale, M_b, and make the evolution to the M_Z scale by using the renormalization group equations. Both ways are equaly valid but the contributions due to the higher order terms enter differently in each procedure because truncated and resummed expressions are used differently. The deviation of the results obtained by means of one or the other method should be regarded as an estimation of the unknown higher order contributions. Taking the average value of both approaches the result obtained for m_b at $\mu = M_Z$ is

$$m_b(M_Z) = 2.67 \pm 0.25 \text{ (stat.)} \pm 0.34 \text{ (frag.)} \pm 0.27 \text{ (theo.)} \; GeV.$$

where the statistical and fragmentation errors correspond to the errors expressed for $R_3^{b\ell}$ in equation 5 and the theoretical error includes the *mass ambiguity* uncertainty (0.25 GeV) and the variation of the scale in the range $0.5 \leq \mu/M_Z \leq 2$ (0.10 GeV).

Another approach to establish the theoretical error is reported in [6]. There, the expression 5 is considered only in terms of the running mass, using the argument that this is a true short distance parameter as opposed to the pole mass which contains all the complicated non-perturbative physics at scales $\mu \sim M_b$. The only error left is then the variation of the scale in the interval from $\mu = 5$ GeV to $\mu = M_Z$. The theoretical error induced by this approach is $\sim$0.20 GeV (+0.10 GeV and -0.30 GeV) due to the fact that the dependence on μ is stronger in this case. The result obtained using this method is $m_b(M_Z) = 2.81$ GeV at $\mu = (M_Z + 5)/2$ which is fully compatible with the above result and constitutes a check of consistency.

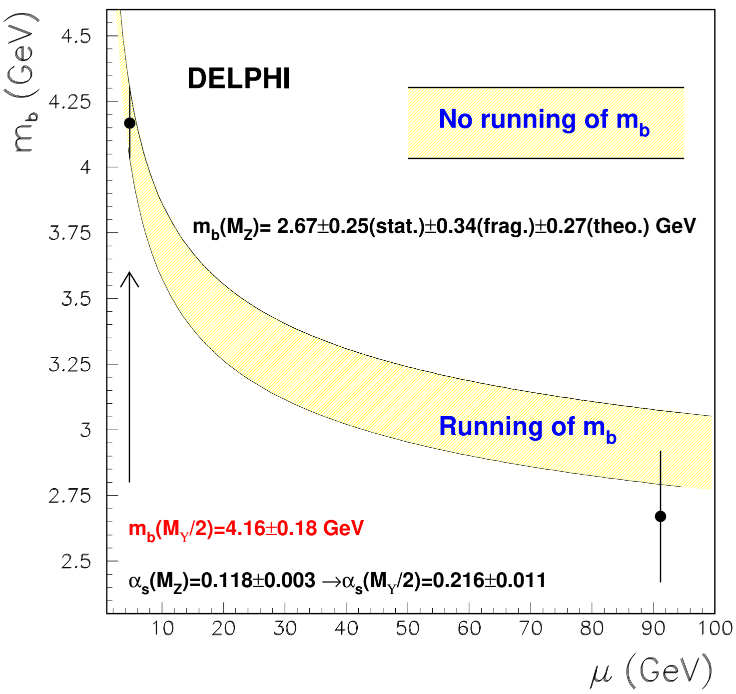

Figure 4: The running of $m_b(\mu)$. The $m_b(M_Z)$ value is displayed only with its statistical error. The grey area quoted *running of* m_b corresponds to the band associated to $m_b(\mu)$ when running the non-weighted average value of $m_b(\mu)$ at $M_\Upsilon/2$ up to the M_Z scale using $\alpha_s(M_Z) = 0.118 \pm 0.003$ [24] and the QCD renormalization group equations.

Assuming all errors were independent, they were added in quadrature and the values of the b running mass at the M_Υ and M_Z scales were compared. The measured difference between them is

$$m_b(M_\Upsilon/2) - m_b(M_Z) = +1.49 \pm 0.52 \; GeV.$$

where the value of $m_b(M_\Upsilon/2) = 4.16 \pm 0.18$ GeV has been calculated as the non-weighted average of all the results appearing in reference [1] at $\mu = M_\Upsilon/2$.

The observed change of the b running mass value from $M_\Upsilon/2$ to M_Z is an effect of almost three standard deviations and represents the first experimental evidence of the running property of any fermion mass. The result is in good agreement with the predicted QCD evolution as is indicated in figure 4 where both mass values are shown together with the two assumptions of running and no-running hypotheses.

Acknowledgements

We are greatly indebted to our technical collaborators and to the funding agencies for their support in building and operating the DELPHI detector, and to the members of the CERN-SL Division for the excellent performance of the LEP collider. We also thank, M. Bilenky, G. Rodrigo and A. Santamaría for what has been in many aspects an enjoyable collaboration plenty of useful and lively discussions on the subject. Furthermore we acknowledge M. Seymour and T. Sjöstrand for their help in understanding the mass effects considered in the HERWIG and JETSET generators.

References

[1] C. A. Dominguez, G. R. Gluckman, N. Paver, Phys. Lett. **B293** (1992), 197 and hep-ph/9410362;
S. Narison, Phys. Lett. **B341** (1994), 73;
M. Neubert, Phys. Report. **245** (1994), 259 and hep-ph/9404296;
S. Titard, F. J. Yndurain, Phys. Rev **D49** (1994), 6007;
M. Jamin, A. Pich, hep-ph/9702276
M.Crisafulli, V. Giménez, G. Martinelli, C.T. Sachrajda, Nucl. Phys. **B457** (1995), 594;
V. Giménez, G. Martinelli, C.T. Sachrajda, Nucl. Phys. Proc. Suppl. **53** (1997), 365 and Phys. Lett. **B393** (1997), 124 ;
C.T.H. Davies et al., Phys. Rev. Lett **D73** (1994), 2654 and Phys. Lett. **B345** (1995) 42.

[2] A. Ballestrero, E. Maina, S. Moretti, Phys. Lett. **B294** (1992), 425 and Nucl. Phys. **B415** (1994), 265.

[3] M. Bilenky, G. Rodrigo, A. Santamaría, Nucl. Phys. **B439** (1995), 505.

[4] DELPHI Coll., P. Abreu et al., Phys. Lett. **307** (1993) 221;
J. Chrin, Proc. 28th Rencontre de Moriond, 1993, p. 313, ed. J.T.T. Van;
J. Valls, PhD Thesis, Universitat de València, 1994, unpublished.

[5] G. Rodrigo, QCD-96 Montpellier, hep-ph/9609213 and Nucl. Phys. Proc. Suppl. **54A** (1997) 60.

[6] M. Bilenky, G. Rodrigo, A. Santamaría, hep-ph/9703358, to be published in Phys. Rev. Lett.

[7] W. Bernreuther, A. Brandenburg, P. Uwer, hep-ph/9703305, to be published in Phys. Rev. Lett.

[8] P. Nason, C. Oleari, CERN-TH-97-092 and hep-ph/9705295.

[9] J. Fuster, S. Cabrera, S. Martí i García, QCD-96 Montpellier, hep-ex/9609004 and Nucl. Phys. Proc. Suppl. **54A** (1997) 39.

[10] DELPHI Coll., P. Aarnio et al., Nucl. Instr. Meth. **A303** (1991) 233;
DELPHI Coll., P. Abreu et al., Nucl. Instr. Meth. **A378** (1996) 57.

[11] S. Catani et al., Phys. Lett. **B269** (1991) 432;
N. Brown, W.J. Stirling, Z. Phys. **C53** (1992) 629.

[12] DELPHI Coll., P. Abreu et al., Z. Phys. **C70** (1996) 179.

[13] ALEPH Coll., D. Buskulic et al., Phys. Lett. **B313** (1993) 535.

[14] G.V. Borisov, DELPHI Internal Note, DELPHI 94-27 PHYS 361 (1994);
G.V. Borisov, Lifetime Tag of Events with B-hadrons with the DELPHI detector, preprint IHEP (Protvino), 94-98 (1994);
DELPHI Coll., P. Abreu et al., Z. Phys. **C65** (1995) 555.

[15] DELSIM user's guide, DELPHI 89-15 PROG 130, CERN, February 1989;
DELSIM Reference Manual, DELPHI 89-68 PROG 143, CERN, September 1989.

[16] T. Sjöstrand, Comp. Phys. Comm. **39** (1986) 346.

[17] DELPHI Coll., P. Abreu et al., Z. Phys. **C73** (1996) 11.

[18] M. H. Seymour, Nucl. Phys. **B436** (1995) 163 and Z. Phys. **C63** (1994) 99;
M.L. Mangano, P. Nason, Phys. Lett **B285** (1992) 160.

[19] K. Hagiwara, T, Kuruma, Y. Yamada, Nucl. Phys. **B358** (1991) 80.

[20] B.L. Ioffe, Phys. Lett. **78B** (1978) 277.

[21] G. Marchesini et al., Comp. Phys. Comm. **67** (1992) 465.

[22] ALEPH Coll., R. Barate et al., CERN-PPE-96-186.

[23] G. Rodrigo, PhD Thesis, Universitat de València, 1996, hep-ph/9703359 and ISBN:84-370-2989-9.

[24] M. Schmelling, ICHEP 96, hep-ex/9701002.